Interleukin-6 (IL-6) receptor/IL-6 fusion protein (Hyper IL-6) effects on the neonatal mouse brain: possible role for IL-6 *trans*-signaling in brain development and functional neurobehavioral outcomes

Susan H. Brunssen[1,2,4], **Sheryl S. Moy**[2], **Arrel D. Toews**[3], **Christopher A. McPherson**[4], and **G. Jean Harry**[4,*]

[1]School of Nursing, University of North Carolina, North Carolina

[2]Carolina Institute for Developmental Disabilities, University of North Carolina, North Carolina

[3]Department of Cellular and Molecular Biology, University of North Carolina, North Carolina

[4]National Toxicology Program Laboratory, National Institute of Environmental Health Sciences, National Institutes of Health, Research Triangle Park, NC

Abstract

Adverse neurodevelopmental outcomes are linked to perinatal production of inflammatory mediators, including interleukin 6 (IL-6). While a pivotal role for maternal elevation in IL-6 has been established in determining neurobehavioral outcomes in the offspring and considered the primary target mediating the fetal inflammatory response, questions remain as to the specific actions of IL-6 on the developing brain. CD-1 male mice received a subdural injection of the bioactive fusion protein, hyper IL-6 (HIL-6) on postnatal-day (PND)4 and assessed from preweaning until adulthood. Immunohistochemical evaluation of astrocytes and microglia and mRNA levels for pro-inflammatory cytokines and host response genes indicated no evidence of an acute neuroinflammatory injury response. HIL-6 accelerated motor development and increased reactivity to stimulation and number of entries in a light/dark chamber, decreased ability to learn to withhold a response in passive avoidance, and effected deficits in social novelty behavior. No changes were observed in motor activity, pre-pulse startle inhibition, or learning and memory in the Morris water maze or radial arm maze, as have been reported for models of more severe developmental neuroinflammation. In young animals, mRNA levels for MBP and PLP/DM20 decreased and less complexity of MBP processes in the cortex was evident by immunohistochemistry. The non-hydroxy cerebroside fraction of cerebral lipids was increased. These results provide evidence for selective effects of IL-6 signaling, particularly *trans-signaling*, in the developing brain in the absence of a general neuroinflammatory response. These data contribute to our further understanding of the multiple aspects of IL-6 signaling in the developing brain.

Keywords

*Corresponding author: G. Jean Harry, Ph.D.; NIEHS, P.O. Box 12233, MD C1-04; Research Triangle Park, NC, 27709 [1 919 541-0927][harry@niehs.nih.gov].

INTRODUCTION

Early inflammatory responses in the fetus and neonate may underlie a diverse range of long-lasting effects on the nervous system (Hagberg and Mallard, 2005). The link between maternal infection and adverse effects in the offspring is thought related to an increased availability of maternal inflammatory factors and induction of a fetal inflammatory response (Cai et al., 2003; Ashdown et al., 2006; Beloosesky et al., 2006; Dammann and O'Shea, 2008). This involves increased production of interleukin (IL)-1, -6, -8, and tumor necrosis factor alpha (TNFα) in chorionic membranes, amniotic fluid, and fetal blood (Fidel et al., 1994; Goepfert et al., 2004). Animal models support neuroinflammation with maternal (Boksa 2010; Gayle et al., 2004; Meyer et al., 2009) or post-natal inflammatory challenge (Cai et al., 2003; Pang et al., 2006) being associated with adverse effects on brain development, myelination (Paintlia et al., 2004; Pang et al., 2003; Loron et al., 2011), and behavior (Shi et al., 2003; Zuckerman et al., 2003; Bilbo et al., 2006; Meyer et al., 2006; Ozawa et al., 2006). In each model, a diverse array of inflammatory responses occurs in the dam or pup. Efforts to tease out critical causative inflammatory factors identified maternal-derived IL-6 as a pivotal factor. In rodent lipopolysaccharide (LPS) models of gestational infection, maternal derived IL-6 contributes to deficits in pre-pulse startle inhibition, latent inhibition and social interactions (Samuelsson et al., 2006; Smith et al., 2007). The nature of the effect shifts with age of exposure (Meyer et al., 2006). Exposure of the postnatal brain to recombinant IL-6 showed did not recapitulate the LPS effects however, the co-administration of an IL-6 neutralizing antibody was effective in blocking the LPS-induced effects (Pang et al., 2006). These findings suggested that, while pivotal, the contribution of IL-6 in developmental neuroinflammation might be related to the level of IL-6R expression induced by co-expressed inflammatory factors.

Interleukin-6 (IL-6) is a pleiotropic cytokine mediating acute-phase responses, cell regeneration, and transition from innate to acquired immunity. The biology of IL-6 is complex with pro- or anti-inflammatory cytokine or neurotrophic actions, depending on the signaling pathway activated (review, Scheller et al., 2011). In the classical pathway, IL-6 binds to a membrane bound IL-6R and the complex associates with gp130, for intracellular signaling. gp130 is present on most neural cells; however, IL-6R expression is restricted in the brain thus, the potential of IL-6 to act through its classical cognate receptor is limited. In trans-signaling, cells expressing only gp130 and lack membrane bound IL-6R can be activated by IL-6/soluble IL-6R (sIL-6R) complex (Jones et al., 2005; Rose-John et al., 2007). Thus, shedding of sIL-6R by neighboring cells upon stimulation as would occur with inflammation and interactions of the IL-6/sIL-6R complex with gp130 provides IL-6 sensitivity to many cell types that do not express IL-6R; expanding biological effects.

Existing data implicating IL-6 in developmental effects of neuroinflammation suggests a role for sIL-6R in subsequent brain damage. However, the existing studies do not address whether an excess of IL-6 in the absence of other inflammatory related factors would produce similar adverse effects. To examine such effects of excess IL-6 trans-signaling, we exposed the early postnatal brain to the bioactive fusion protein, hyper IL-6 (HIL-6), a chimera of recombinant human IL-6 bound to IL-6Rα by a short peptide chain (Fischer et al., 1997). Compared to IL-6/IL-6Rα, HIL-6 has a 100-fold higher receptor binding affinity and while the half-life (approx. 2 hrs) is similar to IL-6, HIL-6 has an enhanced and longer activation of the transcription STAT3-dependent and mitogen-activated protein kinase pathways (Rakemann et al., 1999). We now report direct effects on the developing brain; but unlike the broad spectrum of effects attributed to classical IL-6 signaling with high levels of inflammation, direct subdural exposure of the brain to HIL-6 in post-natal day 4 mice, results in subtle alterations evident in cortical white matter development, motoric development, and long-term effects on reactivity and social behavior.

METHODS

Animals and Hyper IL-6 injection

On postnatal day (PND) 1, [day of birth PND0], litters of 8–12 CD-1 pups (Charles River; Raleigh, NC) were pooled and 10 males were randomly selected and placed with each foster dam. Selected as an age of the developmental transition of OL progenitor cells (pre OLs) to an immature OL, comparable with the human 24–28 weeks of gestation (Craig et al., 2003), PND4 pups were injected with either saline vehicle or HIL-6 on PND4. One-half of the pups were removed and maintained at 35°C. Under cold anesthesia, each pup was visualized on a back-lit stage and, under 2× mag, a 30-g needle was inserted at a 10° angle through the skin and dura overlying the open posterior fontanel (junction of lambdoidal suture and sagittal suture) along the sagittal fissure and 2μl of either phosphate buffered saline (PBS; pH 7.2) vehicle or HIL-6 (5 or 10ng; gift of Stephan Rose-John, Hamburg, Germany) was injected into the subdural cavity over 30sec via a syringe pump. Pups were tattooed, recovered at 35°C (20 min), then returned to the dam and a counterbalanced sequence repeated with remaining pups. Normal maternal/pup interactions and pup survival (1% acute mortality; <1% subsequent morbidity) were maintained. Multiple cohorts of 6 litters were generated with pups assigned to endpoints at injection. With terminal pre-weaning endpoints, age-matched filler mice were used to maintain litter size. At PND21, littermates were housed, one pup/dose, in a semi-barrier animal facility (21°±2°C; 50%±5% humidity; 12-h light/dark cycle). For euthanasia, mice were anesthetized with CO_2, decapitated, the brain excised, and the parietal/temporal cortex and hippocampus dissected (Glowinski and Iverson, 1966) from one hemisphere, rapidly frozen, and stored at −80°C. The contralateral hemisphere was immersion fixed in 4% paraformaldehyde/phosphate buffer pH 7.2 for 18hrs. All procedures complied with UNC/CH and NIEHS/NIH ACUC approved protocols. Dose selection was based upon *in vitro* studies demonstrating activity in HepG2 cells (Peters et al., 1998), neurite outgrowth and branching (Schafer et al., 1999), and induction of glial processes (data not shown). Pilot studies of tracer dye distribution and indications of STAT3 activation from the microarray (Suppl. Fig. 1) suggested delivery of a biologically active substance to the cortex.

Experimental design

In pilot studies, one cohort was used to assess damage from HIL-6 (5 and 10 ng) and to determine age brackets for pre-weaning functional assessments. For terminal endpoints (mRNA analysis, histopathology, protein or lipid analysis), animals were randomly selected from various cohorts. Histopathology, immunohistochemistry, and myelin lipids were examined at both dose levels; given the similarity, data is presented for the 5ng dose. The microarray was conducted at the higher 10ng HIL-6 dose to ensure detection of changes using the less sensitive array procedure. qRT-PCR for myelin specific genes, host response genes and pro-inflammatory cytokines were conducted on the 5ng dose group. Post-weaning assessments were conducted at 5ng HIL-6. The litter determined the n size with only one pup/litter/dose/endpoint.

Preweaning neurodevelopmental assessment

Based upon data from a pilot study (see Suppl. Material), a modified Fox battery (Fox, 1965; Brunssen et al., 2010) was administered on PND8, 12, and 16. Pup weight, nose-rump length, and presence of physical development parameters were recorded. Posture, locomotion, and motor behaviors were observed in an open field. Reflex responses, postural reactions, and strength were assessed. Physical development parameters (vibrissa present, eyelids open, pinna separated, incisors erupted) were scored as absent/present (0,1). Changes in fur distribution [0–4], fur type, posture, locomotion (pivot/crawl, linear/walk), reflexes and postural reactions (cliff aversion, surface or aerial righting, placing responses, fore- and

hind-limb grasp, and auditory startle), kinesthetic response (general fine body tremors) [0–3] and over-generalized response to testing [0–4] were described on ordinal scales. Motor behaviors (sitting, grooming, rearing, running, jumping, and slope exploration) were scored as absent/present (0,1). The pup's ability to grasp a thin metal bar and hold its weight for 15sec max or grasp and climb an inverted wire mesh screen (30 sec max) were measured. Summary scores were created for dichotomously scored variables for physical development (0–4), normal motor (0–3), and heightened motor (0–3) behaviors and analysis restricted to correlations between item scores and HIL-6 level at each age. At PND18 general locomotor activity levels were measured in an open field as sector crosses over 2 min.

Histology and immuohistochemistry

Injury in the cortex and hippocampus was evaluated by hematoxylin and eosin (H&E) staining and immunostaining of astrocytes and microglia. Six-µm paraffin sagittal sections underwent heat-induced epitope retrieval (0.01M citrate buffer pH 6.0; Biocare Medical, Walnut Creek, CA). Sections were blocked with non-immune goat serum (1:50; 10min) prior to 60-min incubation with rabbit anti-cow glial fibrillary acidic protein (GFAP; 1:2000; Dako Corp, Carpinteria, CA), 60 min avidin/biotin reagent (1:100; ABC; Vector Labs, Burlingame, CA), and detected with diaminobenzidine (DAB). Microglia were identified with a rabbit polyclonal antibody to ionized calcium-binding adaptor molecule 1 (Iba-1, 1:500, 1hr, 24°C; Wako Chemicals, Richmond, VA).

mRNA levels for host-response and pro-inflammatory cytokine genes

To evaluate whether the HIL-6 injection resulted in injury and secondary inflammatory response in the cortex, pro-inflammatory and host-response injury genes were examined by RNAse protection assays as previously described (Harry et al., 2003). Within one day of injection (PND5) and at 1-week post-injection (PND11), total RNA was isolated with Trizol™ (Gibco BRL, Gaithersburg, MD). ^{32}[P]-labeled cRNA probe sets contained probes for genes associated with a host-response to injury (Campbell et al., 1994): intercellular adhesion molecule-1 (ICAM-1), inducible nitric oxide synthetase (iNOS), A20 (cytokine-inducible response gene), macrophage-1 antigen (Mac-1), EB22 (acute-phase response gene), and GFAP, or pro-inflammatory cytokines and receptors: IL-1β, IL-1-receptor 1 (IL-1R1), IL-1RII, IL-1 receptor antagonist (IL-1ra), IL-1α, and IL-10; or TNFα, TNFβ, TNF receptor 2 (TNFRp75), TNFR1 (TNFRp55), IL-6Rα, gp130, and IL-6 (BD Pharmingen, San Diego, CA). Relative volume of each ^{32}[P]-fragment was determined from phosphor-imaging (Imagequant; Molecular Dynamics, Sunnyvale, CA) and normalized to corresponding L32.

For the hippocampus, we examined mRNA levels for TNFα, IL-1α, IL-1β, IL-6, and IL-10 mRNA levels at PND5 by qRT-PCR (7900 HT, Applied Biosystems; Foster City, CA) using 2.5µg 77cDNA as template, 1X Power SYBR® Green Master Mix (Applied Biosystems), and forward and reverse primers (Suppl. Table 1). Threshold cycle values were determined from amplification curves, normalized to GAPDH, and mean fold changes over the control group calculated using the comparative C_T method.

Microarray analysis

At PND8 total RNA was isolated from the cortex with Tri-Reagent (Sigma-Aldrich, St. Louis, MO) and purified (Qiagen RNEasy mini-columns; Qiagen, Valencia, CA). Samples (n=3) were pooled from 2 non-littermates and 10µg of cRNA was hybridized to the Affymetrix 430 A 2.0 mouse array (Affymetrix, Sunnyvale, CA; Suppl Material). Data was analyzed by a modified t-statistic, using the observed mean-variance relationship in each sample to construct estimates of group variances (Hu and Wright, 2007). Selection criteria

required a minimum 2-fold change and p<0.01. Pathway analysis and network associations were determined using IPA (Ingenuity Systems, Inc, Redwood City, CA).

Myelin assessment

The mouse forebrain begins to form myelin at approximately PND10-12, preceded a couple of days by an induction of mRNAs related to oligodendrocyte (OL) progenitor cell (OPC) proliferation and myelin proteins. Myelin basic protein (MBP) levels were examined at early accumulation (PND16), peak level of accumulation (PND24), and in the adult (Vincze et al., 2008),

qRT-PCR for myelin related genes—Total RNA was isolated from the cortex (n=12) and 3μg used to generate a 2.5μl cDNA aliquot. Sybr Green PCR Master Mix (Applied Biosystems, Foster City, CA) was used with primers for a marker for oligodendroglia progenitors; integral membrane chondroitin sulfate proteoglycan protein, neuron-glia 2 (NG2) pre-OLs, proteolipid protein (PLP/DM20), late OL maturation and axon contact, myelin associated glycoprotein (MAG), and glyceraldehyde-3-phosphate dehydrogenase (GAPDH) (Suppl. Table 1).

Western blotting—30μg protein was subjected to electrophoresis on 4–12% NuPage® Bis-Tris gels (Invitrogen) and 0.2 μm NuPage® polyvinlyidene difluoride membranes were incubated in rabbit polyclonal anti-MBP (1:2000; 1h, RT; Sigma M3821) then anti-rabbit IgG horseradish peroxidase conjugated antibody (1:50,000; 1h, RT; Santa Cruz Biotech). Membranes were probed with ECL plus (Amersham Biosciences, Arlington Heights, IL) and digital images analyzed (GeneTools version 4.01; Synoptics, Frederick, MD). Membranes were stripped and re-probed with rabbit polyclonal anti-actin (1:5000; 1h, RT; Sigma).

MBP immunohistochemistry—Serial 6μm paraffin sagittal sections were matched for position in the forebrain through the anterior commissure, hippocampal fimbria, and corpus callosum. Sections were blocked with non-immune goat serum (1:50; 10 min), incubated with rabbit anti-MBP (1:500, 20hr, 4°C; Chemicon, Danvers, MA), biotinylated goat anti-rabbit secondary antibody (Chemicon) followed by an AKP ABC complex (Vector Labs, Burlingame, CA), and detected with Nitro-Blue tetrazolium chloride/5-bromo-4-chloro-3′-indolyphosphate p-toluidine salt (NBT/BCIP; Roche, Nutley, NJ).

Lipid extraction and HPLC analysis—Developmental changes in myelin glycolipid synthesizing enzyme follow a rapid increase between PND14 and 20 followed by a stabilization period (Hof and Csiza, 1982). Total lipids were extracted from the forebrain of PND26 mice (n=3) as an early plateau stage, and analyzed by HPLC as previously reported (Muse et al., 2001). Total cerebrosides (hydroxy fatty acid [HFA] and non-hydroxy fatty acid [NFA] galactosyl-ceramides), as well as their sulfated derivatives, sulfatides and cholesterol were expressed as nM/mg tissue weight.

Behavioral assessments

Between PND23 and PND25, individual groups of mice were tested for light/dark place preference, passive avoidance, and pre-pulse startle inhibition (PPI) (San Diego Instruments, San Diego, CA). Adult mice were assessed for motor activity, social behavior and social novelty. Pre-weaning observations were made on all mice. Mice behaviorally-tested as adolescents were not assessed as adults. Any prior testing experience in adults is indicated. The Morris water maze and win-shift radial arm maze assessments were each conducted on independent groups of animals.

Light/Dark place preference—Mice (n=12; PND23) were tested using a modified (white walls in lighted chamber) Gemini II shuttle box to assess activity, anxiety level, and response to a novel environment. Mice were placed in the start chamber, the gate raised and free movement allowed for 10min. The number of entries into the darkened chamber, average duration per dark chamber entry, and total time spent in the dark chamber were recorded.

Passive Avoidance—Mice (n=16–18; PND22-23) received one training session and one test session 24hrs later using a Gemini II shuttle box. Mice were allowed 60sec acclimation to the lighted "safe" side, the gate opened and entry into the dark chamber initiated gate closure and a 3sec scrambled foot shock (0.4mA). The pup remained in the dark compartment for 10sec. This was repeated in the test session. Latency to cross to the dark side was recorded.

Startle and PPI—Mice (n=12; PND25; previously assessed on light/dark test) were assessed for auditory startle response, habituation, and PPI as a measure of sensorimotor gating. Following 5-min habituation, the test session consisted of 42 trials presented with 15-sec variable inter-trial interval (ITI) in blocks of 7 with 70dB background. Session trials were comprised of no-stimulus, acoustic startle stimulus (40msec; 120 dB) alone, and pre-pulse stimulus trials (20msec pre-pulse [4,8,12,16, or 20dB above background], 80msec gap, and 40msec pulse). Startle amplitude was collected across a 65msec sampling-window. PPI was calculated [(1 - response amplitude for prepulse stimulus plus startle stimulus/response amplitude for startle stimulus alone) $\times$ 100].

Locomotor Activity and Rearing—On PND120, mice (n=12) were evaluated for exploratory activity in a photocell activity chamber (40cm $\times$ 40cm $\times$ 30cm). Total ambulatory activity and vertical activity (rearing) were determined in 5-min epochs over a 60-min session.

Social Behavior—At PND140, mice (n=12; previously assessed for activity) were evaluated in a 3-chambered open-access clear plexiglass box to assess social behavior (approach to unfamiliar mouse) and social novelty (preference of a stranger to known mouse). The test consisted of three 10-min phases: habituation, social approach, and social novelty (Moy et al., 2006; Suppl. Material). Time spent in each chamber, number of transitions between chambers, and time spent sniffing wire cage with or without stranger mouse were recorded. Olfactory function was screened by the latency to identify and consume buried novel food (Froot Loops, Kellogg, Battle Creek, MI).

Radial Arm Maze (RAM)—On PND80, mice (n=6) were acclimated to handling and chocolate-flavored food pellets (Bioserve, Frenchtown, NJ). Following overnight food restriction, each mouse freely explored a baited maze until all 8 pellets were retrieved within 300sec (4–5 sessions). To assess working and reference spatial memory, acquisition of the win-shift task (win food, shift to new location) over 15 daily 5-min sessions with each arm baited (Levin et al., 2004). Pellet retrieval, number of baited arms entered until the mouse made an error and reentered a prior arm, latency per entry, and a measure of random choice (proportion incorrect = # incorrect arms/total # arms entered) were recorded by two observers at >90% inter-rater reliability. Trials with fewer than five arms entered were considered failed trials. Animals were maintained at 80% free-feeding body weight.

Morris water maze (MWM)—At PND180, mice (n=12; previously assessed for activity) were assessed for spatial learning and reference memory. A water-habituation trial was followed by 4, 1-min trials/day (10-min ITI) over 4 days, to learn location of a submerged

platform. Latency to find the platform, swimming distance, and swimming velocity were recorded (Noldus Ethovision, Leesburg, VA). On day 5, a 1-min probe trial was conducted. A 4-trial retention test was conducted 17 days later followed by 4 days of reversal learning of a different platform location.

Statistical analysis

Spearman's Rank Order Correlation for cross-sectional measures tested ordinal variables in the neurodevelopment assessment. Within-subject repeated measures (weight, length, RAM) were tested using General Linear Mixed Models (SAS). Repeated Measures ANOVAs were used for locomotor activity, PPI, and MWM. Light-dark place preference and MWM probe trial were analyzed by Student's *t*-tests and passive avoidance by Mann-Whitney U. Cerebroside and cholesterol levels were analyzed by one-way ANOVAs. RPAs and qRT-PCR data were analyzed by ANOVAs for treatment, age, and interaction effects. Post-hoc pairwise comparisons were made by Fisher's PLSD or Student's *t* test with Bonferroni correction following a significant overall ANOVA or HIL-6 main effect. Significance was set at p 0.05.

RESULTS

Acute histological response to HIL-6 injection

Histological examination of the brain within the first week following injection confirmed the absence of an injury response due to the procedure or to HIL-6. In the cortex, a few eosin+ cells could be observed within localized areas and was considered within the normal control range (Suppl. Fig. 2A). GFAP staining of astrocytes displayed cells with thin ramified processes (Suppl. Fig. 2B) and Iba-1 microglia showed no evidence of activation (Suppl. Fig. 3). No HIL-6 induced changes in H&E, GFAP, or Iba-1 were observed in the hippocampus (Suppl. Fig. 4) or any other brain regions located within the plane of cut.

Observation assessments during pre-weaning development

No differences were seen in body weight, length, or brain weight (data not shown). In the pilot study, age-dependent appearances of physical developmental landmarks were similar across groups. HIL-6 mice demonstrated earlier onset of straight line walking, earlier loss of cliff aversion, later onset of coordinated forelimb grasp and elevated motor reactivity to sensory stimulation and handling (Suppl. Table 2). In the subsequent cohorts, these findings were confirmed. Compared to controls, HIL-6 mice showed persistence of hyperkinesias at PND12 (Fig. 1A). On PND8, control mice maintained an immature pivot locomotor response [Spearman's $\rho_{(34)}= -0.339$, *p*=0.047] (Fig. 1B); while, HIL-6 mice showed an earlier onset of straight line walking [$\rho_{(34)}=0.334$, *p*=0.05] (Fig. 1C). Developmental onsets of spontaneous motor behaviors (sitting, grooming, rearing) were similar across groups (Fig. 1D). Heightened motor activities in HIL-6 mice showed a general trend for increase frequency across PND12 [$\rho_{(34)}=0.303$, *p*=0.076] and PND16 [$\rho_{(35)}=0.421$, *p*=0.011] (Fig. 1E). Increased general reactivity to handling was observed at PND8 [$\rho_{(34)}=0.523$, *p*=0.001], PND12 [$\rho_{(34)}=0.519$, *p*=0.001], and PND16 [$\rho_{(35)}=0.465$, *p*=0.004] (Fig. 1F). An exacerbated startle response was observed in HIL-6 mice at PND12 [$\rho_{(34)}=0.483$, *p*=0.003] and PND16 [$\rho_{(35)}=0.394$, *p*=0.019] (Fig. 1G). At PND 18 no significant difference was observed in open-field activity level (data not shown).

qRT-PCR of inflammatory-related cytokines in the hippocampus

Consistent with the absence of a microglia response in the hippocampus, qRT-PCR indicated no significant differences in mRNA levels for TNFα, IL-1α, IL-1β, IL-6 while mRNA levels for IL-10 showed a significant increase in the HIL-6 mice at PND5 (Fig. 2).

Lack of elevated inflammatory cytokine mRNA in the cortex

To evaluate whether an acute cellular injury and associated inflammatory response was induced by the HIL-6 injection during the first week, RPAs were conducted on cortical tissue at PND5 and 11 (24hr and 1wk post-injection). Significant age effects were seen for MAC-1 [$F_{1,6}$ =15.65, p=0.007] and EB-22 [$F_{1,6}$= 21.7, p=0.003] (Fig. 3A). mRNA levels for IL-1RII, IL-1Ra, IL-10 (Fig. 3B), TNFα, and TNFβ (Fig. 3C) were similar across age. IL-1β showed a slight increase at both ages in the HIL-6 dose group however, it failed to reach statistical significance. Significant increases between PND5 and 11 were detected for IL-1R1 [$F_{1,17}$ = 6.28, p = 0.023], IL-1α [$F_{1,17}$ = 18.61, p<0.001] (Fig. 3B), TNFRp55 [$F_{1,15}$ = 16.63, p=0.014], gp130 [$F_{1,15}$=32.62, p=0.001], and IL-6 [$F_{1,15}$ = 20.5, p=0.001] (Fig. 3C). No HIL-6 treatment related effects were detected (Fig. 3A–C).

Microarray analysis of cortex

Samples examined at PND8, 96 hrs post-HIL-6 injection, showed altered levels for a number of mRNA transcripts. Criteria for selecting genes required a minimum of 2-fold change with p<0.01. Consistent with the RPA analysis there was no indication of an inflammatory response initiated by HIL-6. A total of 1164 mapped genes were altered, 373 were lower and 791 were higher. Since we were examining for all of the significant functions in the dataset, we used a Benjamini-Hochberg multiple testing correction and the glutamate receptor signaling and the axonal guidance signaling pathways emerged as the top canonical pathways affected. The genes showing the highest level of fold-change in the HIL-6 mice compared to controls were molecules of diverse function (Table 1). Data indicated that the injection of HIL-6 induced an elevation in genes associated with activation of the STAT3 signaling pathway (Fig. 4A). With regards to myelin related genes, the microarray profile suggested a change in genes related to OL maturation and myelination as indicated by network linkage via MBP (Fig. 4B). HIL-6 did not alter mRNA levels for chondroitin sulfate proteoglycan, a marker for early neuroglia precursors, nor NG2. Myelin-associated oligodendrocyte basic protein (MOBP) was decreased by 2.8 fold. This was accompanied by a 7.9-fold decrease in MBP and a 3.7-fold decrease in myelin proteolipid protein (PLP). mRNA levels for enzymes involved in lipid hydroxylation and turnover and believed to be uniquely expressed in OLs, fatty acid-2 hydroxylase, UDP-galactosyltransferase, as well as Ugt8a were decreased in the HIL-6 mice.

qRT-PCR for myelin genes in the cortex

When we examined mRNA levels for selected myelin related genes by qRT-PCR (Fig. 5A), no changes were observed in the marker for OL precursors, NG2, from PND5 to 16. PLP and its alternatively spliced isoform DM20 are main intrinsic membrane proteins of compact myelin with essentially identical mRNA developmental profiles (LeVine et al., 1990). Similar to changes observed in PLP in the microarray, qRT-PCR mRNA levels for PLP/DM20 were decreased 0.6 to 0.8 fold across all three ages in HIL-6 mice (main effect for HIL-6 [$F_{1,27}$ =6.2, p=0.02]; post-hoc analysis showed a significant decrease at PND24 [t_9=3.04; p=0.014]. For MAG, a protein developmentally associated with late OL maturation and signaling between the axon and myelin (McKerracher et al., 1994), mRNA levels increased 1.3 to 1.5 fold and a significant main effect of HIL-6 was observed across the developmental window [$F_{1,28}$ =4.44, p=0.045; Fig. 5A].

HIL-6 increased NFA-cerebroside fraction

Cerebroside (galactosyl-ceramide; GalC) is a major myelin component providing a rapid and sensitive index of myelin deposition, with a peak rate of deposition and ceramide galactosyltransferase mRNA expression between 3–4 weeks of age (Muse et al., 2001). Total cerebroside levels were not significantly different between groups. The control levels

of sulfatides (57+7 nM/mg tissue wt) and HFA-cerebrosides (38±6 nM/mg tissue wt), as percent of total cerebrosides, were not significantly altered by HIL-6. The NFA-cerebroside fraction was significantly increased (2.5-fold) in HIL-6 mice (Fig. 5B, [$F_{2,6}$=7.28; p=0.025]) resulting in a decreased ratio of HFA:NFA-cerebrosides (controls: 7.88; HIL-6: 2.3). Total cholesterol was not altered (control: 18.4+3.4 nM/mg tissue weight; HIL-6; 17.9±2.0 nM/mg; p=0.98).

Myelin Basic Protein

Protein levels of MBP showed a normal increase across development from PND16 to adult by both Western blot and immunohistochemistry. Western blots showed no indication that HIL-6 exposure decreased the total amount of MBP (data not shown). However, the pattern of MBP staining indicated differences. Myelinated tracts were detected within the corpus callosum, cortex, and fine linear processes within the frontal lobe at PND16 (Fig. 5C). In the HIL-6 mice, staining in the corpus callosum suggested a denser packing of myelinated fibers with approximately 25% +/− 5% decrease in width. Myelinated projections into the cortex visually displayed less branching complexity (Fig. 5C; Suppl. Fig. 5). At PND24, MBP staining was not as compact in the corpus callosum as observed at PND16 and no differences in width were detected. An age-related increase in complexity of the myelinated fibers within the cortex was observed in both groups (Fig. 5D). Visual representation suggested a diminished level of complexity of myelinated processes in the HIL-6 mice (Fig. 5D). This was especially evident in the projections from the corpus callosum to the cortex. The overall evaluation of the frontal lobe suggested a similar effect; however, this was variable across animals and showed no specific deficit in HIL-6 mice. In the adult, MBP staining was similar between the HIL-6 mice and controls with a further increase in process complexity occurring with maturation; however, we were unable to visually detect a change in HIL-6 mice (data not shown).

HIL-6 altered behavioral performance

Light/dark place preference—HIL-6 mice showed a significant increase in the number of entries into the dark chamber [t_{20}=3.8; p=0.003] (Fig. 6A) and duration from each entry was significantly less as compared to controls [t_{14}=3.14; p=0.004] (Fig. 6B).

Passive avoidance—Passive avoidance examines the ability to learn to inhibit a normal escape response and invokes higher cortical circuits involving modulation of emotion and fear responses to adverse stimuli. In the initial training session for passive avoidance, no difference was observed in the latency to enter the preferred dark chamber as a function of HIL-6 administration (Fig. 6C). In the test session, HIL-6 dosed mice showed a significant deficit with a lower latency to enter the dark chamber [Mann-Whitney U= 61; p=0.0009 one-tailed] (Fig. 6C) suggesting a hindered ability to learn to withhold this normal response.

Pre-pulse startle inhibition—Startle amplitude to 120 dB stimulus (Fig. 7A) did not differ between controls and the HIL-6 mice [$F_{1,21}$= 1.35, p=0.258]. Both showed the expected reduction in amplitude across increasing prepulse levels [$F_{5,110}$= 58.43, p<0.0001] (Fig. 7B). Amplitudes in HIL-6 mice were maintained at 17% above controls but did not reach statistical significance [$F_{1,110}$= 1.05; p=0.307]. Both groups showed the expected change in PPI across increasing prepulse levels [$F_{4,88}$=56.95; p<0.0001] but no significant difference between controls and HIL-6 mice was observed [$F_{1,88}$=0.22; p=0.644].

Social behavior—Social approach behavior was not altered by HIL-6. All mice showed normal preference for the stranger mouse versus an empty cage in presence time in chamber with stranger [p<0.05] (Fig. 8A) and time spent sniffing the stranger [p<0.001] (Fig. 8B). In the test for social novelty, control mice showed a preference for the newly introduced

stranger, spending approximately 35% greater time in this chamber and a significant increase in time spent sniffing stranger 2 [t_{11}=3.17, p<.01] (Fig. 8C,D). HIL-6 injected mice failed to demonstrate a preference for stranger 2 on either measure (Fig. 8C,D). Latency to find novel buried food indicated intact olfactory function in both groups (data not shown).

Locomotor activity—Locomotor activity levels were similar across groups. All mice showed a normal pattern of habituation across the 60-min test session in both distance travelled and number of rearing events (Fig. 9A–B).

Morris Water Maze—Total acquisition, latency to find platform during training, was not significantly altered by HIL-6 (Fig. 9C). In the probe trial, all adult mice showed a significantly greater proportion of time spent in the target quadrant [p<0.05] (Fig. 9D). No differences were observed for swimming distance or in swimming velocity during the test sessions (data not shown). When mice were tested for the ability to shift their response to a new quadrant, no significant difference was observed between the HIL-6 treated mice and controls in the latency to find the platform in the 4-day reversal task (Fig. 9E).

Radial-arm maze—Mice exposed to HIL-6 did not differ significantly from controls in acquisition of the 8-arm radial-maze task. In both groups, the mean number of consecutive correct choices prior to making an error increased from 4 (random) to a peak performance of 7 after 10 days of training ($F_{1,165}$=23.1, p<0.0001). The proportion of incorrect choices declined from 40% to ~20% for both groups by day 10 ($F_{1,165}$=11.2, p=0.007). As a general pattern, the acquisition of speed for arm choices (latency/entry) differed by HIL-6 treatment over the 15 training sessions ($F_{1,154}$=4,70, p=0.032; HIL-6 by day quadratic interaction; GLM). HIL-6 mice displayed a more rapid latency (mean=20 sec) than controls (mean=27 sec) during the initial sessions. Both groups achieved maximum speed (~9sec) following one week of training ($F_{1,153}$=0.05, p=0.82).

DISCUSSION

Recent work suggests IL-6 as a critical factor for altered neurodevelopment associated with early-life inflammation; however, it is also suggested that effects attributed to IL-6 may be dependent upon co-expression of other inflammatory factors or the developmental window of exposure. We now demonstrate that early postnatal exposure of the brain to HIL-6, in the absence of elevations in TNFα and IL-1 or neuronal death, produces subtle changes in specific aspects of neurobehavior. This is in contrast to the broad effects previously attributed to IL-6 under more severe inflammatory conditions. HIL-6 mice displayed a premature emergence of locomotor responses and motoric responses and elevated reactivity to environmental stimuli. Deficits in place preference and passive avoidance were observed in juvenile mice and a reduced preference for social novelty in adults. Unlike previous studies, no alterations were found in motor activity and spatial learning and memory performance with the exception of a more rapid initial training latency in the RAM. Subtle changes were observed in oligodendroglia and myelin specific genes and NFA-cerebroside fraction during the pre-weaning and adolescent period with no evidence of a decrease in myelin basic protein but a slight transient alteration in the complexity of myelinated processes suggesting an effect on the developing OL similar to previous observations in perinatal infection models (Roberson et al., 2006).

The majority of earlier studies demonstrating a profound impact of gestational infection on offspring behavior utilized models with elevated maternal inflammatory factors and reported a disruption in a number of neurobehavioral endpoints (Samuelsson et al., 2006; Smith et al., 2007; Ito et al., 2010). These studies not only represent an earlier time in brain development as compared to the current study but also a more severe and broad-spectrum inflammatory

response as they examined acute/sub-acute relatively high-dose LPS effects. The vulnerability of the brain and specific cellular targets can change with development; however, neurotoxicity from LPS is not necessarily dependent upon gestation as a time of exposure as similar effects in rodents have been observed with postnatal exposure. Given that IL-6 has been considered the primary cytokine involved in these responses, Pang et al. (2006) compared effects of exposure to IL-6 with those following LPS and found no similar manifestation of neurotoxicity. However, upon co-administration of IL-6 neutralizing antibody, the LPS effect was attenuated, suggesting a dependency upon interactions with other LPS-related factors to stimulate IL-6R expression or shedding of soluble IL-6R for biological activity. It can be speculated that involvement of sIL-6R may account for the differences observed within the literature with regards to the contribution of IL-6 to neurodevelopmental effects. Signaling via the IL-6/sIL-6R complex under inflammatory conditions would be similar to HIL-6 in that it would be active on cells that did not normally express IL-6R. One major difference would be that, with HIL-6, signaling would occur in the absence of other inflammatory factors or microglia activation. Thus, using HIL-6 allowed us to identify the unique contribution of IL-6 to these neurodevelopmental alterations. If indeed, an acute exposure of the developing brain to IL-6 signaling can produce alterations in behaviors that are often associated with human neurodevelopmental disorders, as seen in the current study, this raises a level of clinical concern for lower levels of exposure than previously considered. A further understanding is needed of the contribution of trans-signaling versus classical IL-6 signaling to neurodevelopmental inflammation and subsequent behavioral alterations. It is possible that as a natural inhibitor to prevent IL-6/sIL-6R complex from interacting with membrane-bound gp130 (Heinrich et al., 2003), soluble gp130 could potentially be used to elucidate such contributions. This would then allow for the further evaluation of sIL-6R as a potential therapeutic target for early post-natal immune-mediated response in the brain.

The selective behavioral impairments found in the present study suggest that exposure to HIL-6 led to alterations in the developmental trajectory, with improvement emerging in adulthood. In the present study, neonatal HIL-6 mice exhibited transition from pivoting to straight-line walking at a significantly earlier age than controls, suggesting the possibility of a similar accelerated maturation of motor areas. Something similar was observed in an LPS model of intrauterine inflammation in the rat with offspring showing an earlier proficiency of forelimb placement and surface righting than controls (Poggi et al. 2005) and in improved motor performance in a postnatal LPS inflammatory rat model for cerebral palsy (Roberson et al., 2006). Alterations in the developmental trajectory of the cortex have also been identified in humans. For example, the longitudinal assessment of children with attention-deficit/hyperactivity disorder (ADHD) has revealed general delays in cortical maturation yet, accelerated maturation in the primary motor cortex (Shaw et al. 2010).

The neonatal and adolescent HIL-6 mice exhibited several phenotypes in line with impaired development of response inhibition and impulse control, including increased activity in the light/dark task, hyper-reactivity to handling and acoustic stimuli, and decreased latencies in the passive avoidance task. However, few abnormal behaviors were observed in the adult HIL-6 mice. In a non-human primate model of moderate self-limiting bacterial infection induced by LPS (2ng/kg/iv on GD 125 and 126), IL-6 levels over 2 days were only moderately elevated yet at 2 months of age, these animals displayed a heightened level of responsiveness (Willette et al., 2011). In ADHD, delayed maturation of the anterior cingulate, striatum, and medial temporal lobes has been associated with age-dependent deficits in response inhibition (McAlonan et al. 2009). Shaw et al. (2010) found that the most severe maturational delay in ADHD was in the lateral prefrontal cortex, another brain region thought to be important for impulse control. The early behavioral abnormalities in the

HIL-6 mice could reflect a similar shift in maturation of higher-order cortical regions critical for appropriate response inhibition.

One aberrant phenotype observed in the adult HIL-6 mice was a loss of social novelty preference, without changes in sociability. Motivation in the social novelty task includes a general preference for social proximity and a more specific preference for social novelty, as well as the ability to discriminate between a newly introduced stranger and an already-investigated stranger. Thus, performance in this phase of the task reflects more complex motivation and demands than the sociability phase. Several genetic mouse models for neurodevelopmental disorders have selective deficits in social novelty preference (Moy et al. 2009; O'Tuathaigh et al. 2007; Pietropaolo et al. 2011; Radyushkin et al. 2009). Hemispheric connectivity might be especially important for responses during complex social encounters that involve rapid information processing across different brain regions and have been implicated in human neurodevelopmental disorders associated with altered social behavior (Minshew and Williams, 2007). In the present study, exposure to HIL-6 led to age-dependent reductions in the width of the corpus callosum and complexity of myelinated fibers, which may be relevant to the disruption of complex social behavior observed in the current study.

It has been hypothesized that myelin deficits observed following developmental inflammation are due to oligodendrocyte progenitor cell damage. Cai et al. (2003) speculated that a loss of OL progenitors contributed to the deficit in MBP on PND8 following maternal rat LPS exposure on GD18 -19. Further work suggested that LPS-activated microglia induced OL cell death and impaired OL development (Pang et al., 2010). Delayed cell death was attenuated with blocking TNFα activity and the impaired development by ciliary neurotrophic factor (CNTF). Marmur et al (1998) demonstrated that density-dependent potentiation of OL maturation is mediated by environmental signals such as cytokines that activate gp130/leukemia inhibitory factor β receptors and CNTF. In this regard, IL-6 signaling has been associated with early differentiation OLs that may shift the process of myelination. For example, IL-6R/IL-6 chimera protein induced cultured pre-OL differentiation into mature oligodendroglia, promoted survival, and increased the number of highly arborized OLs (Valerio et al., 2002) potentially due to premature cell-cycle exit and early differentiation of OL progenitors (Zhang et al., 2004). Similar results have been reported *in vivo* with intracervical injections of LPS (0.1 mg/kg) on GD15 promoting generation of OPCs (Poggi et al., 2005). In contrast to the Pang et al (2010) study, the direct administration of HIL-6 did not activate microglia nor did it elevate TNFα, suggesting an absence of the LPS-mediated mechanisms for OPC death. Rather, it is of greater likelihood that the injection of HIL-6 on PND4 facilitated premature differentiation of OPCs, shifting the normal pattern of myelination. In addition to the direct actions on cultured OLs (Valerio et al., 2002), HIL-6 promotes neurotrophin expression in astrocytes (März et al., 1999) that may in turn promote OL maturation. An alternative or additional player is the activation of glutamate receptor signaling as this was detected as a top canonical pathway identified in HIL-6 mice and both glutamate and N-methyl-D-aspartate stimulate stem cell OL differentiation promoting maturation and myelination (Cavaliere et al., 2012).

Premature maturation of OLs could alter the accurate matching of myelin segments to axonal surfaces. Given the role of MAG to facilitate axon/OL interactions, elevated MAG mRNA seen during pre-weaning may represent an earlier induction of myelination that could be indicative of or influence OL maturation. The gene encoding PLP is expressed in mature OLs but also in OPCs (Gudz et al., 2006) and the protein can function in cell migration (Fulton et al., 2010). Thus, changes observed in PLP mRNA levels in the HIL-6 mice may also represent changes in OL development and migration along the axon. A functional shift in OLs is also suggested by changes in the non-hydroxylated fatty acid

(NFA)-cerebroside sub-fraction of myelin as a specific enzymatic pathway particular to immature cerebral OLs (Hof and Csiza, 1982). The specific increases in the NFA-cerebroside sub-fraction and reductions in FA2H and CGT mRNA levels observed with HIL-6 suggest altered enzyme activity for alpha-hydroxylation of fatty acids and/or turnover of galactosphingolipids in cerebral OLs. Alternatively, the mRNA pattern and the decreased myelin process complexity could represent a change in the underlying axon.

These results contribute to our understanding of the complex interactive nature of the inflammatory response in the developing brain. We now demonstrate the potential for IL-6 to mediate selective effects on the post-natally developing brain in the absence of systemic immune responses, induction of a pro-inflammatory cytokine cascade, or cell death. The pattern of changes suggests a role for IL-6 signaling in influencing the establishment of social and environmental interactive patterns for use later in life. Whether this can be linked to reactivity and social behavioral changes observed in animal models of neurodevelopmental disorders is an area for future research.

Supplementary Material

Refer to Web version on PubMed Central for supplementary material.

Acknowledgments

References

Ashdown H, Dumont Y, Ng M, Poole S, Boksa P, Luheshi GN. The role of cytokines in mediating effects of prenatal infection on the fetus: implications for schizophrenia. Mol Psychiatry. 2006; 11:47–55. [PubMed: 16189509]

Beloosesky R, Gayle DA, Amidi F, Nunez SE, Babu J, Desai M, Ross MG. N-acetyl-cysteine suppresses amniotic fluid and placenta inflammatory cytokine responses to lipopolysaccharide in rats. Am J Obstet Gynecol. 2006; 194:268–273. [PubMed: 16389042]

Bilbo SD, Rudy JW, Watkins LR, Maier SF. A behavioural characterization of neonatal infection-facilitated memory impairment in adult rats. Behav Brain Res. 2006; 169:39–47. [PubMed: 16413067]

Boksa P. Effects of prenatal infection on brain development and behavior: a review of findings from animal models. Brain Behav Immun. 2010; 24:881–897. [PubMed: 20230889]

Brunssen, SH.; Moy, SS.; Kissling, GE. Principles of Behavioral Phenotyping in Neonatal and Adult Mice. In: Harry, GJ.; Tilson, HA., editors. Neurotoxicology, Target Organ Toxicology Series. 3. New York: Informa Healthcare; 2010. p. 283-308.

Cai Z, Pang Y, Lin S, Rhodes PG. Differential roles of tumor necrosis factor-alpha and interleukin-1 beta in lipopolysaccharide-induced brain injury in the neonatal rat. Brain Res. 2003; 975:37–47. [PubMed: 12763591]

Campbell IL, Eddleston M, Kemper P, Oldstone MB, Hobbs MV. Activation of cerebral cytokine gene expression and its correlation with onset of reactive astrocyte and acute-phase response gene expression in scrapie. J Virol. 1994; 68:2383–2387. [PubMed: 8139024]

Cavaliere F, Urra O, Alberdi E, Matute C. Oligodendrocyte differentiation from adult multipotent stem cells is modulated by glutamate. Cell Death Dis. 201210.1038/cddis.2011.144

3 A, Luo NL, Beardsley DJ, Wingate-Pearse N, Walker DW, Hohimer AR, Back SA. Quantitative anlaysis of perinatal rodent oligodendrocyte lineage progression and its correlation with human. Exp Neurol. 2001; 181:231–240.

Dammann O, O'Shea M. Cytokines and perinatal brain damage. Clinics in Perinatology. 2008; 35:643–663. [PubMed: 19026332]

Fidel PL Jr, Romero R, Wolf N, Cutright J, Ramirez M, Araneda H, Cotton DB. Systemic and local cytokine profiles in endotoxin-induced preterm parturition in mice. Am J Obstet Gynecol. 1994; 170:1467–1475. [PubMed: 8178889]

Fischer M, Goldschmitt J, Peschel C, Brakenhoff JPG, Kallen KJ, Wolimer A, Grotzinger J, Rose-John S. A designer cytokine with high activity on human hematopoietic progenitor cells. Nat Biotechnol. 1997; 15:142–145. [PubMed: 9035138]

Fox WM. Reflex-ontogeny and behavioural development of the mouse. Animal Behavior. 1965; 13:234–241.

Fulton D, Paez PM, Campagnoni AT. The multiple roles of myelin protein genes during the development of the oligodendrocyte. ASN NEURO. 2010; 2(1):art:e00027.10.1042/AN20090051

Gayle DA, Beloosesky R, Desai M, Amidi F, Nunez SE, Ross MG. Maternal LPS induces cytokines in the amniotic fluid and corticotropin releasing hormone in the fetal rat brain. Am J Physiol Regul Integr Comp Physiol. 2004; 286:R1024–R1029. [PubMed: 14988088]

Glowinski J, Iversen LL. Regional studies of catecholamines in the rat brain-I: The disposition of [3H]norepinephrine, [3H]dopamine and [3H]D)PA in various regions of the brain. J Neurochem. 1966; 13:655–669. [PubMed: 5950056]

Goepfert AR, Andrews WW, Carlo W, Ramsey PS, Cliver SP, Goldenberg RL, Hauth JC. Umbilical cord plasma interleukin-6 concentrations in preterm infants and risk of neonatal morbidity. Am J Obstet Gynecol. 2004; 191:1375–1381. [PubMed: 15507968]

Gudz TI, Komuro H, Macklin WB. Glutamate stimulates oligodendrocyte progenitor migration mediated via an $\alpha\varpi$ integrin/myelin proteolipidprotein complex. J Neurosci. 2006; 26:2458–2466. [PubMed: 16510724]

Hagberg H, Mallard C. Effect of inflammation on central nervous system development and vulnerability. Curr Opin Neurol. 2005; 18:117–123. [PubMed: 15791140]

Harry GJ, Bruccoleri A, Lefebvre d'Hellencourt C. Differential modulation of hippocampal chemical-induced injury response by ebselen, pentoxifylline, and TNFalpha-, IL-1 alpha-, and IL-6-neutralizing antibodies. J Neurosci Res. 2003; 73:526–536. [PubMed: 12898537]

Heinrich PC, Behrmann I, Haan S, Hermanns HM, Müller-Newen G, Schaper F. Principles of interleukin (IL)-6-type cytokine signaling and its regulation. Biochem J. 2003; 374:1–20. [PubMed: 12773095]

Hof L, Csiza CK. Developmental changes in glycolipid synthesizing enzymes in the brain of a myelin-deficient mutant Wistar rat. J Neurochem. 1982; 39:1434–1439. [PubMed: 6214615]

Hu J, Wright FA. Assessing differential gene expression with small sample sizes in oligonucleotide arrays using a mean-variance model. Biometrics. 2007; 63:41–19. [PubMed: 17447928]

Ito HT, Smith SE, Hsiao E, Patterson PH. Maternal immune activation alters nonspatial information processing in the hippocampus. Brain Behav Immun. 2010; 24:930–941. [PubMed: 20227486]

Jones S, Richards PJ, Scheller J, Rose-John S. IL-6 transsignaling: the in vivo consequences. J Interferon Cytokine Res. 2005; 25:241–253. [PubMed: 15871661]

Levin ED, Brunssen S, Wolfe GW, Harry GJ. Neurobehavioral assessment of mice after developmental AZT exposure. Neurotox Teratol. 2004; 26:65–71.

LeVine SM, Wong D, Macklin WB. Developmental expression of proteolipid protein and DM20 mRNAs and proteins in the rat brain. Dev Neurosci. 1990; 12:235–250. [PubMed: 1705207]

Loron G, Olivier P, See H, Le Saché N, Angulo L, Biran V, Brunelle N, Besson-Lescure B, Kitzis MD, Pansiot J, Bingen E, Gressens P, Bonacorsi S, Baud O. Ciprofloxacin prevents myelination delay in neonatal rats subjected to E. coli sepsis. Ann Neurol. 2011; 69:341–351. [PubMed: 21387379]

März P, Heese K, Dimitriades-Schmutz B, Rose-John S, Otten U. Role of interleukin-6 and soluble IL-6 receptor in region-specific induction of astrocytic differentiation and neurotrophin expression. Glia. 1999; 16:191–200. [PubMed: 10340760]

Marmur R, Kessler JA, Zhu G, Gokhan S, Mehler MF. Differentiation of oligodendroglial progenitors derived from cortical multipoint cells requires extrinsic signals including activation of gp130/LIFbeta receptors. J Neurosci. 1998; 18:9800–9811. [PubMed: 9822739]

McAlonan GM, Cheung V, Chua SE, Oosterlaan J, Hung SF, Tang CP, Lee CC, Kwong SL, Ho TP, Cheung C, Suckling J, Leung PWL. Age-related grey matter volume correlates of response inhibition and shifting in attention-deficit hyperactivity disorder. Br J Psychiatry. 2009; 194:123–129. [PubMed: 19182173]

McKerracher L, David S, Jackson DL, Kottis V, Dunn RJ, Braun PE. Identification of myelin-associated glycoprotein as a major myelin-derived inhibitor of neurite growth. Neuron. 1994; 13:805–811. [PubMed: 7524558]

Meyer U, Feldon J, Fatemi SH. In-vivo rodent models for the experimental investigation of prenatal immune activation effects in neurodevelopmental brain disorders. Neurosci Biobehav Rev. 2009; 33:1061–1079. [PubMed: 19442688]

Meyer U, Nyffeler M, Engler A, Urwyler A, Schedlowski M, Knuesel I, Lee BK, Feldon J. The time of prenatal immune challenge determines the specificity of inflammation-mediated brain and behavioral pathology. J Neurosci. 2006; 26:4752–4762. [PubMed: 16672647]

Minshew NJ, Williams DL. The new neurobiology of autism: cortex, connectivity, and neuronal organization. Arch Neurol. 2007; 64:945–950. [PubMed: 17620483]

Moy SS, Nadler JJ, Magnuson TR, Crawley JN. Mouse models of autism spectrum disorders: the challenge for behavioral genetics. Am J Med Genet C Semin Med Genet. 2006; 142C:40–51. [PubMed: 16419099]

Moy SS, Nonneman RJ, Ghashghaei HT, Weimer JM, Yokota Y, Lee D, Lai C, Threadgill DW, Anton ES. Deficient NRG1-ERBB signaling alters social approach: relevance to genetic mouse models of schizophrenia. Journal of Neurodevelopmental Disorders. 2009; 1:302–312. [PubMed: 21547722]

Muse ED, Jurevics H, Toews AD, Matsushima GK, Morell P. Parameters related to lipid metabolism as markers of myelination in mouse brain. J Neurochem. 2001; 76:77–86. [PubMed: 11145980]

O'Tuathaigh CM, Babovic D, O'Sullivan GJ, Clifford JJ, Tighe O, Croke DT, Harvey R, Waddington JL. Phenotypic characterization of spatial cognition and social behavior in mice with 'knockout' of the schizophrenia risk gene *neuregulin 1*. Neuroscience. 2007; 147:18–27. [PubMed: 17512671]

Ozawa K, Hashimoto K, Kishimoto T, Shimizu E, Ishikura H, Iyo M. Immune activation during pregnancy in mice leads to dopaminergic hyperfunction and cognitive impairment in the offspring: a neurodevelopmental animal model of schizophrenia. Biol Psychiatry. 2006; 59:546–554. [PubMed: 16256957]

Paintlia MK, Paintlia AS, Barbosa E, Singh I, Singh AK. N-acetylcysteine prevents endotoxin-induced degeneration of oligodendrocyte progenitors and hypomyelination in developing rat brain. J Neurosci Res. 2004; 78:347–361. [PubMed: 15389835]

Pang I, Cai Z, Rhodes PG. Disturbance of oligodendrocyte development, hypomyelination and white matter injury in the neonatal rat brain after intracerebral injection of lipopolysaccharide. Dev Brain Res. 2003; 140:205–214. [PubMed: 12586426]

Pang Y, Fan LW, Zheng B, Cai Z, Rhodes PG. Role of interleukin-6 in lipopolysaccharide-induced brain injury and behavioral dysfunction in neonatal rats. Neurosci. 2006; 141:745–755.

Pang Y, Campbell L, Zheng B, Fan L, Cai Z, Rhodes P. Lipopolysaccharide-activated microglia induced death of oligodendrocyte progenitor cells and impede their development. Neurosci. 2010; 166:464–475.

Peters M, Blinn G, Solem F, Fischer M, zum Buschenfelde KHM, Rose-John S. In vivo and in vitro activities of the gp130-stimulating designer cytokine hyper-IL-6. J Immunology. 1998; 161:3575–3581. [PubMed: 9759879]

Pietropaolo S, Guilleminot A, Martin B, D'Amato FR, Crusio WE. Genetic-background modulation of core and variable autistic-like symptoms in *FMR1* knock-out mice. PLoS One. 2011; 6:e17073. [PubMed: 21364941]

Poggi SH, Park J, Toso L, Abebe D, Roberson R, Woodard JE, Spong CY. No phenotype associated with established lipopolysaccharide model for cerebral palsy. J Obstet Gynecol. 2005; 192:727–733.

Radyushkin K, Hammerschmidt K, Boretius S, Varoqueaux F, El-Kordi A, Ronnenberg A, Winter D, Frahm J, Fischer J, Brose N, Ehrenreich H. *Neuroligin-3*-deficient mice: model of a monogenic heritable form of autism with an olfactory deficit. Genes Brain Behav. 2009; 8:416–425. [PubMed: 19243448]

Rakemann T, Niehof M, Kubicks S, Gischer M, Manns MP, Rose-John S, Trautwein C. The designer cytokine Hyper-interleukin-6 is a potent activator of STAT3-dependent gene transcription in vivo and in vitro. J Biol Chem. 1999; 274:1257–1266. [PubMed: 9880494]

Roberson R, Woodard JE, Toso L, Abebe D, Poggi SH, Spong CY. Postnatal inflammatory rat model for cerebral palsy: Too different from humans. Amer J Obstetrics Gynecol. 2006; 195:1038–1044.

Rose-John S, Waetzig GH, Scheller J, Grötzinger J, Seegert D. The IL-6/sIL-6R complex as a novel target for therapeutic approaches. Expert Opin Ther Targets. 2007; 11:613–624. [PubMed: 17465721]

Samuelsson AM, Jennische E, Hansson HA, Holmang A. Prenatal exposure to interleukin-6 results in inflammatory neurodegeneration in hippocampus with NMDA/GABA(A) dysregulation and impaired spatial learning. Am J Physiol Regul Integr Comp Physiol. 2006; 290:R1345–R1356. [PubMed: 16357100]

Schafer KH, Mestres P, Marz P, Rose-John S. The IL-6/sIL-6R fusion protein hyper-IL-6 promotes neurite outgrowth and neuronal survival in cultured enteric neurons. J Interferon Cytokine Res. 1999; 19:527–532. [PubMed: 10386865]

Scheller J, Chalaris A, Schmidt-Arras D, Rose-John S. The pro- and anti-inflammatory properties of the cytokine interleukin-6. Biochim Biophys Acta. 2011; 1813:878–888. [PubMed: 21296109]

Shaw P, Gogtay N, Rapoport J. Childhood psychiatric disorders as anomalies in neurodevelopmental trajectories. Human Brain Mapping. 2010; 31:917–925. [PubMed: 20496382]

Shi L, Fatemi SH, Sidwell RW, Patterson PH. Maternal influenza infection causes marked behavioral and pharmacological changes in the offspring. J Neurosci. 2003; 23:297–302. [PubMed: 12514227]

Smith SEP, Li J, Garbett K, Mirnics K, Patterson PH. Maternal immune activation alters fetal brain development through interleukin-6. J Neurosci. 2007; 27:10695–10702. [PubMed: 17913903]

Valerio A, Ferrario M, Dreano M, Garotta G, Spano P, Pizzi M. Soluble interleukin-6 (IL-6) receptor/ IL-6 fusion protein enhances in vitro differentiation of purified rat oligodendroglial lineage cells. Mol Cell Neurosci. 2002; 21:602–615. [PubMed: 12504593]

Vincze A, Mázló M, Seress L, Komoly S, Abrahám H. A correlative light and electron microscopic study of postnatal myelination in the murine corpus callosum. Int J Devel Neurosci. 2008; 26:575–584. [PubMed: 18556167]

Willette AA, Lubach GR, Knickmeyer RC, Short SJ, Styner M, Gilmore JH, Coe CL. Brain enlargement and increased behavioral and cytokine reactivity in infant monkeys following acute prenatal endotoxemia. Behav Brain Res. 2011; 219:108–115. [PubMed: 21192986]

Zhang P, Chebath J, Lonai P, Revel M. Enhancement of oligodendrocyte differentiation from murine embryonic stem cells by an activator of gp130 signaling. Stem Cells. 2004; 22:344–354. [PubMed: 15153611]

Zuckerman L, Rehavi M, Nachman R, Weiner I. Immune activation during pregnancy in rats leads to a postpubertal emergence of disrupted latent inhibition, dopaminergic hyperfunction, and altered limbic morphology in the offspring: a novel neurodevelopmental model of schizophrenia. Neuropsychopharmacology. 2003; 28:1778–1789. [PubMed: 12865897]
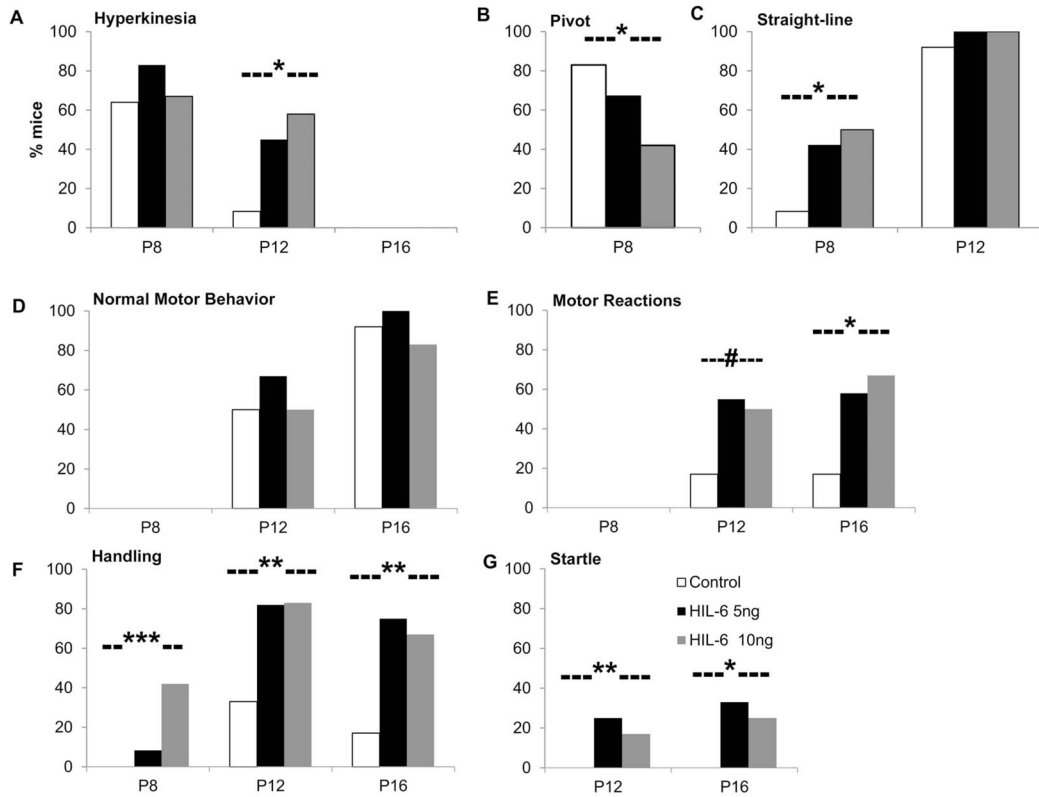
Figure 1.
Summary scores of preweaning neurobehavioral assessment. (A) hyperkinesias [0–3]. (B) pivot locomotor reaction to stimulation. (C) early emergence of straight-line locomotion. (D) Normal motor behaviors. (E) heightened motor reactions (running, jumping, leaping, stereotypic air sniffing). (F) General reactivity to handling. (G) reaction to startle stimulus. Bars represent % of mice (n=12/post-natal (P) age/group) exhibiting selected behaviors. Spearman's Rank Order correlation for HIL-6 dose (0, 5, 10 ng) by scale score (range 0–3 or 0–4) within post-natal age; #$p<0.10$, *$p<0.05$, **$p<0.01$, ***$p<0.001$.
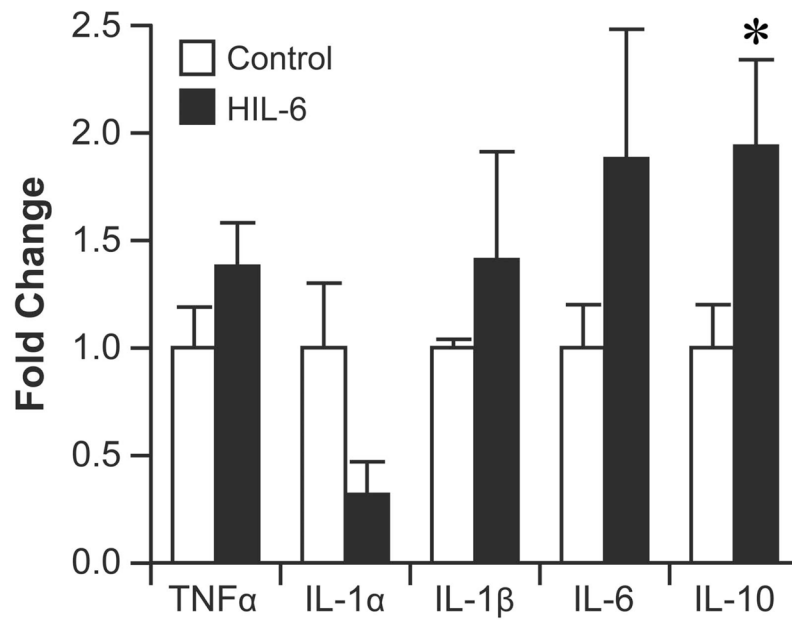
Figure 2.
Quantitative real-time PCR (qRT-PCR) for cytokines in the hippocampus. Mice were injected with vehicle (white bar) or HIL-6 (5ng; dark bar) at PND4 and tissue collected at PND5. Data are presented as mean fold increase (±SEM) over the average control value for each transcript. *significantly different from controls $p<0.05$.

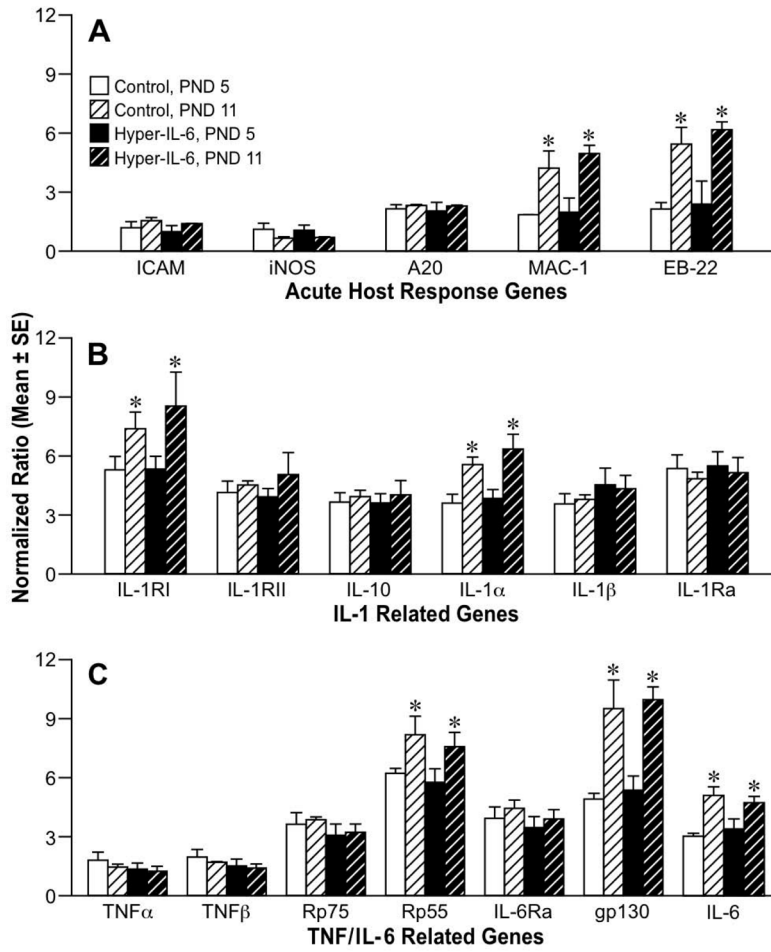**Figure 3.**
RNase protection assay for (A) acute response genes and inflammatory cytokines ICAM-1, iNOS, A20, MAC-1 and EB22 (B) Interleukin 1 related genes and (C) TNF and IL-6 related genes on total RNA isolated from cortex at PND5 and 11 from mice injected with vehicle or HIL-6 5ng at PND4. Values represent normalized mean ratio of pixel volume determined by phosphor-imaging for each transcript (± SE) to corresponding L32. *Significantly different across age within exposure group, p<0.05.
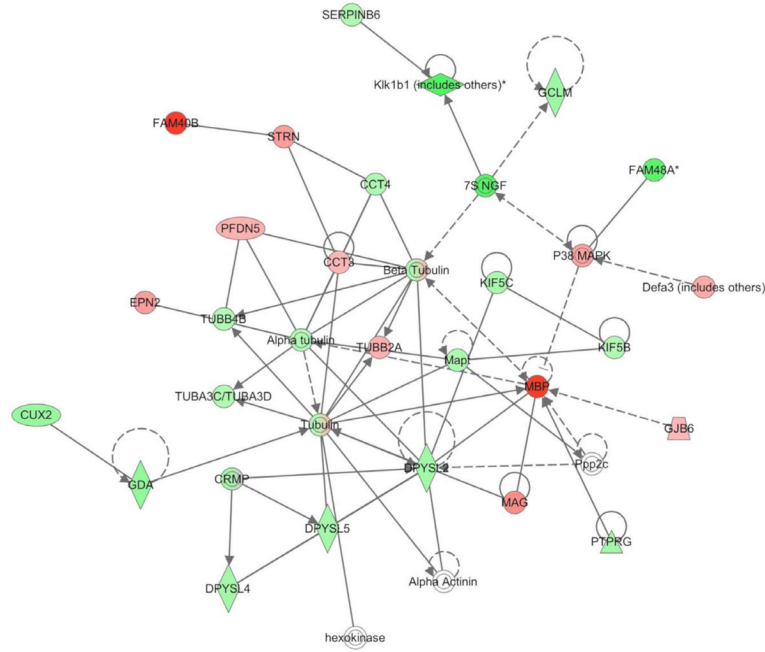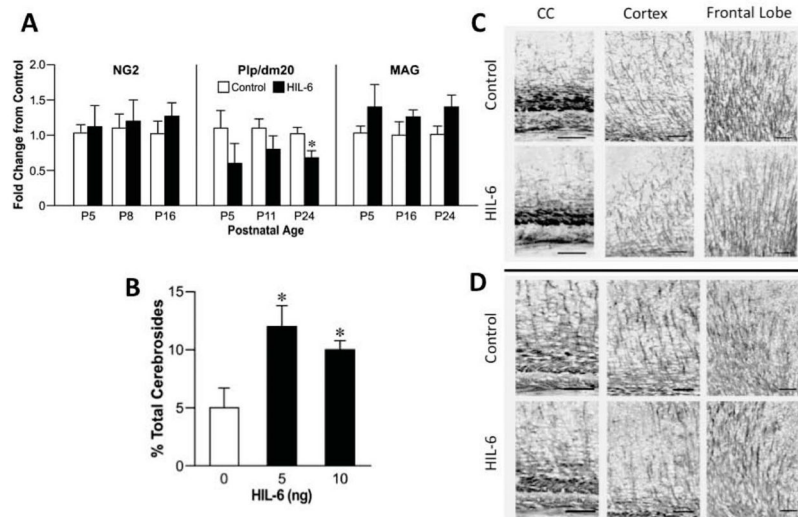
Figure 4.
Ingenuity IPA network association of microarray analysis changes in gene transcripts related to MBP in the cortex at PND8 as altered by PND4 HIL-6 exposure. Red indicates down-regulated (FAM40B, STRN, PFDN5, EPN2, CCT3, TUBB2A, P38MAPK, Defa3, GJB6, MAG, MBP) and Green indicates up-regulated, with no change in hexokinase, Alpha Actinin, Ppp2c. Symbols are derived from Ingenuity network analysis: ⬭transcription regulator ⬯transporter ◎ complex/group ○other ⬩enzyme ◆ peptidase

Figure 5.
(A) qRT-PCR for myelin specific transcripts in the cortex at various postnatal days (P) relevant to the developmental profile of each: NG2 (P5, 8, 16), PLP/DM20 (P5, 11, 24), and MAG (P5, 16, 24) of mice injected at P4 with vehicle (white bars) or 5ng HIL-6 (dark bars). ANOVA indicated a main effect of HIL-6 for PLP/DM20 and MAG. *significant post-hoc analysis with Bonferroni correction for multiple comparisons (p=0.014) as compared to vehicle. (B) NFA cerebrosides as a percent of total cerebrosides (NFA-cerebroside fraction) in adult mice injected at PND4 with either vehicle or HIL-6 (5 ng). Data represents the mean % value ± SEM. *significantly different from controls ($p<0.05$).
(C–D) Representative photomicrographs of immunostaining for myelin basic protein (MBP, 1:500, 20hr, 4°C) as detected by NBT/BCIP. Staining intensity and complexity of MBP myelin tracts increased with age (C: PND16 [Suppl. Fig. 5]; D: PND24). Branch points observed in the HIL-6 mice suggested less complexity of myelinated fibers.
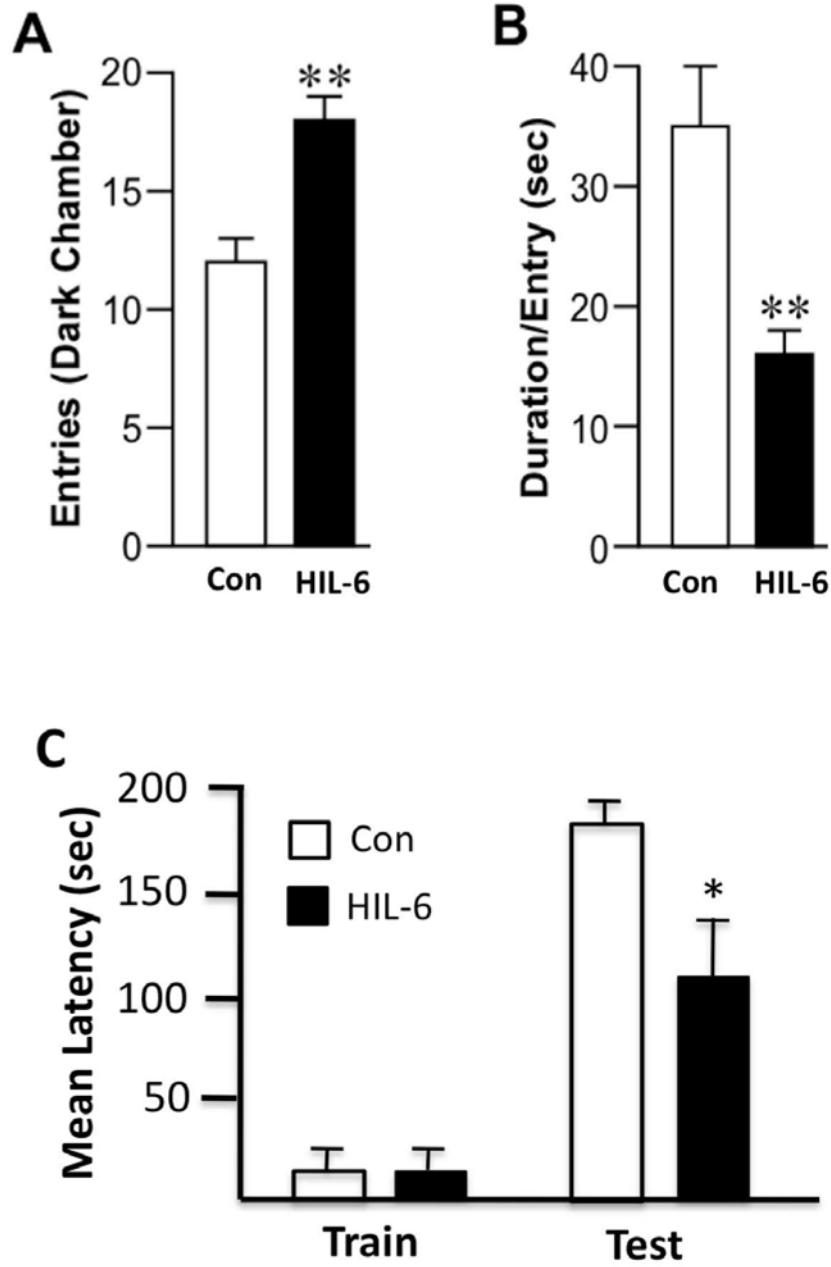
Figure 6.
(A–B) Light/dark place preference. (A) Number of entries into the dark chamber over a 10-min test session. (B) Mean duration (sec) per individual entry. Data represents mean ± SEM. (C) Passive avoidance performance. Data represents the mean ± SEM latency to enter the dark chamber on test day. Con – white bars; 5 ng HIL-6 -dark bars *statistically significant from control *p<0.05; ** p<0.01.
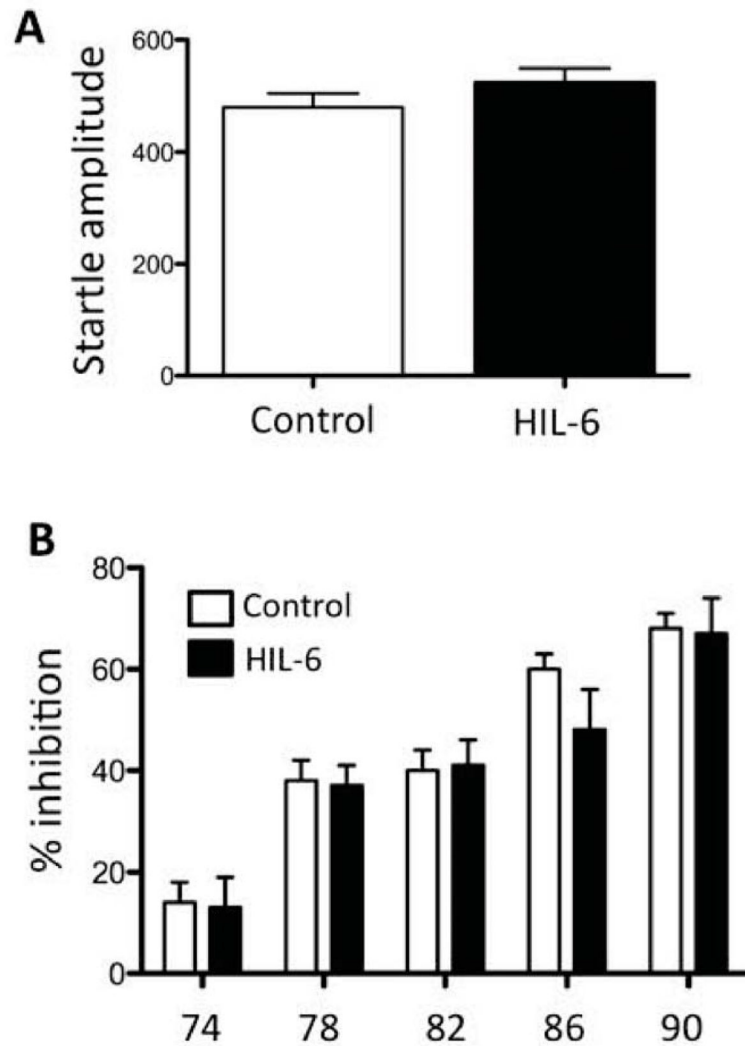
Figure 7.
(A) Startle response amplitude in PND25 mice injected at PND4 [Control – white bar; HIL-6 5 ng – dark bar]. Data represents the mean over 6 trials. (B) Pre-pulse startle inhibition across pre-pulse stimulus intensities. Data represent the mean ± SEM.
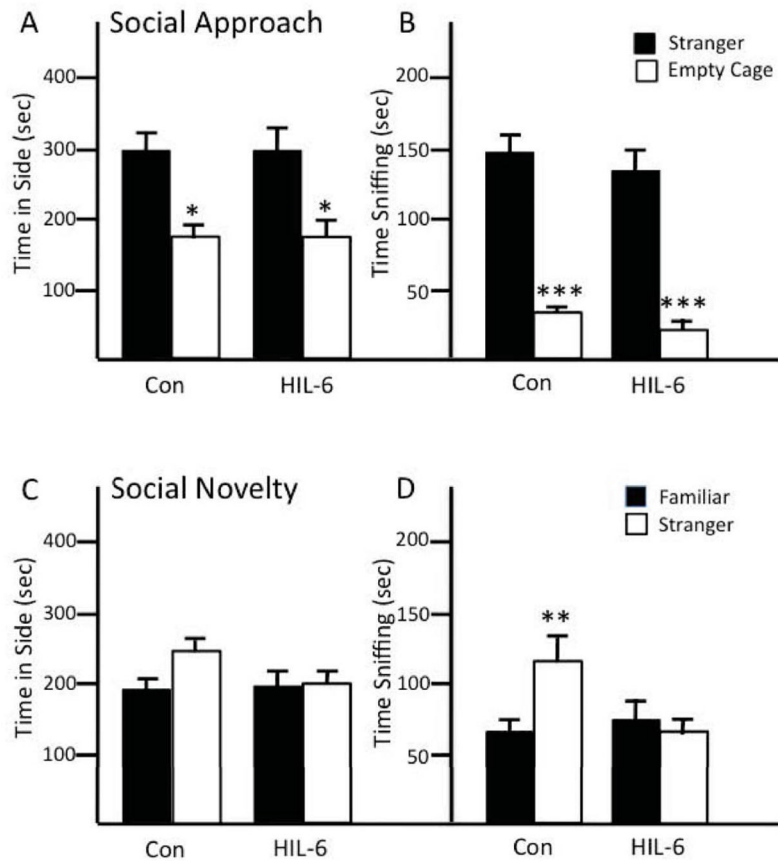
Figure 8.
Social behavior of adult mice injected with vehicle (Con) or HIL-6 (5ng) on PND4. Social
Approach: (A) total time (sec) spent in contact with (B) sniffing unfamiliar mouse compared
to empty wire cage. Social Novelty: (C) total time (sec) spent in contact with (D) sniffing
familiar mouse compared to stranger. Data shown are mean ± SEM (n=12). *p<0.05;
**p<0.01; ***p<0.001 statistical difference between stranger and empty cage or familiar
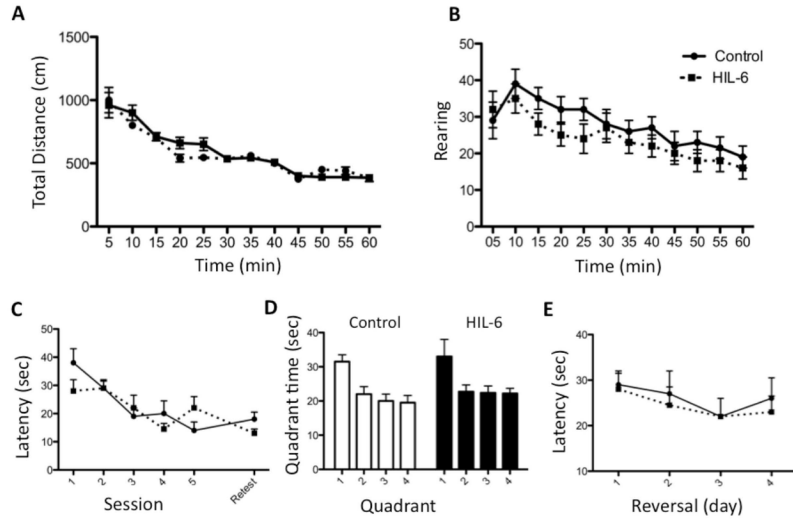and stranger mouse within control and HIL-6 groups.

Figure 9.
Motor activity (A,B) and MWM (C,D) in adult mice injected on PND4 with vehicle (Control) or 5ng HIL-6. (A) Total ambulation distance (cm) travelled (B) number of rears occurring during 5-min epochs for 60 min. Data represent mean ± SEM. (C) Latency to find hidden platform across 5 days of training. Data shown are mean ± SEM of 4 trials/day. (D) Probe trial - % time (of 1-min) spent in each quadrant. (E) Reversal - latency to find hidden platform. Data shown are means ± SEM of 4 trials per session.

TABLE 1

Microarray Analysis of Cortex

Top Canonical Pathways	p-value[a]	Ratio[b]
Glutamate Receptor Signaling	0.00038	11/69
Axonal Guidance Signaling	0.00095	39/430

TOP MOLECULES

Up-Regulated	Fold-Change[c]
KDM5B – lysine (K)-specific demethylase 5B	8.26
PRPF4B – alcohol group acceptor phosphotransferase, snRNP	7.93
BECN1 – beclin 1, autophagy related	7.91
STK4 – serine/threonine kinase 4	7.84
BAZ1A – bromodomain adjacent to zinc finger domain, 1A	7.63
ROBO3 – roundabout, axon guidance receptor, homolog 3	7.18
CYP – cytochrome P450, family 7, subfamily B, polypeptide 1	6.99
PISD - phosphatidylserine decarboxylase	6.90
IKBKB - inhibitor of kappa light polypeptide gene enhancer in B-cells, kinase β	6.60
MESDC2 – mesoderm development candidate 2	6.30

Down-Regulated	Fold-Change
FAM40B – family with sequence similarity 40, member B	9.15
MBP – myelin basic protein	7.75
PDE10A – 3′,5′-cyclic-nucleotide phosphodiesterase, Pde	7.08
ARPC3 – actin related protein 2/3 complex, subunit 3, 21kDa	7.05
LMO4 – LIM domain only 4	6.80
SLC35D3 – solute carrier family 35, member D3	6.75
SEMA7a – semaphoring 7A, GPI membrane anchor	6.58
CAMK2A – calcium/calmodulin-dependent protein kinase II alpha	6.48
MID1 – midline 1	6.07
GNG7 – G protein beta gamma	5.69

[a] Canonical pathways were determined by Ingenuity using Benjamini-Hochberg multiple testing correction to determine p value.

[b] The ratio represents the number of focused molecules as a function of the total number of molecules in that process.

[c] Fold change relative to vehicle control.